

Sensory Glove-Based Surgical Robot User Interface

Leonardo Borgioli^{1*}, Ki-Hwan Oh^{1*}, Alberto Mangano², Alvaro Ducas², Luciano Ambrosini², Federico Pinto², Paula A López², Jessica Cassiani², Miloš Žefran¹, Liaohai Chen² and Pier Cristoforo Giulianotti²

Abstract—Robotic surgery has reached a high level of maturity and has become an integral part of standard surgical care. However, existing surgeon consoles are bulky and take up valuable space in the operating room, present challenges for surgical team coordination, and their proprietary nature makes it difficult to take advantage of recent technological advances, especially in virtual and augmented reality. One potential area for further improvement is the integration of modern sensory gloves into robotic platforms, allowing surgeons to control robotic arms directly with their hand movements intuitively. We propose one such system that combines an HTC Vive tracker, a Manus Meta Prime 3 XR sensory glove, and God Vision wireless smart glasses. The system controls one arm of a da Vinci surgical robot. In addition to moving the arm, the surgeon can use fingers to control the end-effector of the surgical instrument. Hand gestures are used to implement clutching and similar functions. In particular, we introduce clutching of the instrument orientation, a functionality not available in the da Vinci system. The vibrotactile elements of the glove are used to provide feedback to the user when gesture commands are invoked. A preliminary evaluation of the system shows that it has excellent tracking accuracy and allows surgical fellows to efficiently perform standard surgical training tasks with minimal practice with the new interface; this suggests that the interface is highly intuitive. The proposed system is inexpensive, allows for rapid prototyping, and opens opportunities for further innovations in the design of surgical robot interfaces.

I. INTRODUCTION

Robotic surgery has reached a high level of maturity and has become an integral part of standard surgical care. For the surgeon, it offers increased precision and dexterity through efficient interaction interfaces. However, despite its high acceptance and success, it faces some challenges in modern operating rooms. The surgeon consoles are bulky and take up valuable space [1]. A redesigned workspace promises to improve turnaround time, increase throughput, and reduce cost [2]. Studies further emphasize the potential of ergonomic workspace design and nonoperative process redesign to advance the efficiency of robotic surgical devices [3], [4]. Another challenge with current consoles is that the surgeon is separated from the rest of the team, which can lead to challenges in communication [5] and can impact the efficiency of the operational workflow in tasks such as robotic docking [6]. Finally, the proprietary nature of existing consoles makes it difficult to innovate in this space despite

rapid advances in fields such as augmented and virtual reality that could benefit the surgeon.

Several studies have attempted to address some of these shortcomings. [7] proposes a novel method for controlling the endoscope through a head-mounted master interface (HMI) integrated with a surgical robot system. [8] controls the surgical robot arm and the Augmented Reality (AR) interface through various hand gestures. In [5], the authors provide a nice review of existing approaches and opportunities.

One potential area for further improvement and technological innovation in robotic surgery is the integration of modern sensory gloves into robotic platforms, which allows surgeons to intuitively control robotic arms with their hand movements without the need for additional manipulators that are customary for existing consoles. Furthermore, most end-effectors of surgical robot instruments, such as the Fenestrated Bipolar Forceps (FBF) and the Large Needle Driver (LND), are limited to the use of opposing blades due to the design of the console manipulators (as the last joint is controlled only by pinching two fingers); glove-based control could offer the surgeon additional dexterity while using these instruments.

Glove-based control is intuitive and is popular in robotics applications outside the surgical field. For instance, a low-cost wireless system with a glove equipped with bending sensors is described in [9]. In [10], the authors demonstrate glove-based control in rehabilitation, using gloves equipped with Inertial Measurement Units (IMUs) for patient exercises. Glove-based control for telemanipulation tasks, integrating force sensors for enhanced feedback, is explored in [11]. These studies explore various sensor modalities and develop communication techniques and control algorithms to achieve sophisticated and effective glove-based control systems for robotic arms.

In our work, we develop a system in which an HTC Vive Tracker [12] is attached to a Manus Meta Prime 3 Haptic XR sensory glove [13], equipped with multiple IMUs and bending sensors for finger tracking, to control one arm of the da Vinci surgical robot paired with the da Vinci Research Kit (dVRK) [14]; the visual feedback to the surgeon is provided through God Vision wireless smart glasses [15]. In addition, this setup manipulates the robotic arm's end effector (jaw of the instrument) through finger movements. Moreover, we implemented hand gesture recognition to substitute pedal inputs of the current da Vinci console (e.g. clutch). This also allows us to clutch the instrument orientation, a functionality not provided by the da Vinci system. The glove is equipped

*First two authors contributed equally to this work.

¹Robotics Lab, Department of Electrical and Computer Engineering, College of Engineering, University of Illinois Chicago, Chicago, IL 60607, USA.

²Surgical Innovation and Training Lab, Department of Surgery, College of Medicine, University of Illinois Chicago, Chicago, IL 60607, USA.

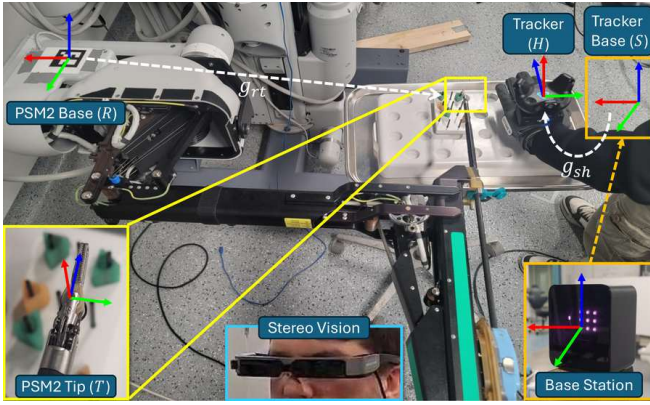


Fig. 1: The setup showing the configuration of the da Vinci arm (PSM) and the Manus glove with the HTC Vive Tracker attached. The user wears the God Vision smart glasses for the stereo endoscopic view. Shown are the x (red), y (green), and z (blue) axes of the relevant coordinate frames.

with vibrotactile elements to provide feedback to the user about whether the gesture is activated.

We evaluate the proposed system in terms of tracking accuracy and the ability of the user to perform surgical training tasks similar to those used in training with the da Vinci devices. The evaluation shows that the system is responsive and that surgeons can effectively complete training exercises with minimal practice with the new interface, suggesting that the interface is highly intuitive. The proposed system is inexpensive as it uses off-the-shelf components and it dramatically reduces space requirements. It demonstrates how modalities such as vibrotactile feedback can efficiently provide additional information to the surgeon without cluttering the visual field. Finally, the proposed architecture allows for rapid prototyping and opens opportunities for further innovations in the design of surgical robot interfaces.

II. METHODOLOGY

A. System Architecture

The system integrates several components. The surgical robot platform consists of the first-generation da Vinci robot paired with the dVRK. One of the Patient Side Manipulators (PSMs) is equipped with the Fenestrated Bipolar Forceps (FBF) instrument and is subject to glove control. The arm is configured as in Fig. 1. The HTC Vive Tracker attached to the Manus glove provides the pose of the hand, while the fingers are tracked by the Manus Meta Prime 3 XR. In addition, classifier models were trained for hand gesture recognition; hand gestures were used to supersede da Vinci’s pedal inputs. The visual feedback to the user is provided through God Vision smart glasses. The system runs the Robot Operating System (ROS) [16] that facilitates seamless communication and coordination between the Manus glove, the HTC Vive Tracker, and dVRK, ensuring real-time data streaming and responsive interaction between the user and the control interface. The architecture allows for easy prototyping.

B. da Vinci Arm Kinematics

For the full da Vinci system, the kinematic chain from the Patient Side Manipulator (PSM) tip to the Endoscope Camera Manipulator (ECM) tip involves Setup Joints (SUJs). The poses provided by the dVRK exhibit errors within a range of $\pm 5\text{cm}$ for translation and fall between $5 \sim 10$ degrees for orientation. These inaccuracies arise due to challenges in calibrating the SUJs precisely, as reported in [14]. Consequently, we implemented a custom calibration method for the dVRK using fiducial markers [17] that eliminates the influence of SUJs and allows us to accurately determine the transformation between the PSM base (frame R) and the instrument tip (frame T) (Fig. 1).

C. Glove Kinematics

To monitor the glove’s position and orientation within the environment, we attached an HTC Vive Tracker to it. The glove’s position and orientation data are updated at 120 Hz using the data from the IMUs and HTC Vive Base Stations [18], [19].

The coordinate frames for the HTC Vive Tracker and Base Station are depicted in Fig. 1. At initialization, the tracker frame H and the tracker base frame S coincide and are aligned with the PSM instrument tip frame T . A displacement of H from S results in the scaled motion of PSM (see below) to create an intuitive control for the user.

D. Control Architecture

To ensure safety for both the glove and the instrument tip, we define their operational workspaces to be cubes, with a larger side L_h for the glove and a side L_t for the instrument tip, centered at their initial positions. In both cases, movements beyond the cube volume are projected to the cube surface.

The movements of the glove tend to be significantly larger than the desired movements of the PSM tip ($L_h > L_t$). The motion of the glove is thus scaled to match the range needed for PSM operations:

$$\Delta p_t = \eta \Delta p_h \quad (1)$$

where Δp_h represents the translational movement of the glove from its initial position, and Δp_t denotes the expected translational movement of the PSM from its initial position, and $\eta = L_t/L_h$ is the scaling factor. Similarly to the existing surgeon console, the scaling factor η can be adjusted.

E. Finger Tracking

The tracking of the relative transformation between the fingers and the wrist is accomplished using the five sets of flexible sensors with 2 Degrees of Freedom (DoF) and six sets of 9 DoF IMUs of the Manus Meta Prime 3 Haptic XR glove, operating at a rate of 90Hz. These sensors boast a $\pm 2.5^\circ$ accuracy [13]. The glove software provides a hand skeleton mesh, inspired by the Mediapipe framework [20]. This mesh is dynamically adjusted based on the readings from the glove sensors, allowing for a real-time representation of the hand pose.

In our architecture, the Euclidean distance between the tips of the index and thumb fingers is used to control the jaw of the end effector. To map the distance of the fingers to the distance between the tips of the jaw we use an expression analogous to Eq. (1). This enables precise and intuitive control of the robotic system.

F. Hand Gesture Recognition

Hand gestures serve as a seamless and intuitive means of interaction and open up the possibility of introducing a large variety of inputs that can surpass what the current consoles can provide. For example, in [8] it was shown that it is possible to implement 8 different commands.

In our work, we train 4 different multiclassification models for hand gesture recognition using our custom dataset. Our implemented architecture can currently distinguish between five distinct gestures: **None**, **Pinky** (thumb and pinky in contact), **Ring** (ring finger and thumb in contact), **Fist**, and **Thumb up**, as illustrated in Table I. Our framework allows a new gesture to be added in just a few minutes. Currently, only three of the five gestures serve as commands (**Fist**, **Ring**, and **Pinky**). **Fist** activates the clutch mechanism, **Ring**, if held for 2 seconds, initiates and suspends robot tracking, and **Pinky** triggers monopolar current delivery [21]. See Section III for further details.

G. Clutch

The clutch functionality in the da Vinci surgical robot serves as a safety feature and a means of control for the surgeon during robotic-assisted surgeries. This mechanism essentially allows the surgeon to recenter the workspace of the surgeon console by temporarily disengaging the movement of the robotic arms while still maintaining control of the Master Tool Manipulators.

When the surgeon operates the da Vinci system’s master console, which consists of hand and finger controls, they can engage or disengage the clutch as needed. This allows them to stop the movement of the robotic arms, enabling them to make adjustments or reposition the controllers as required during the procedure.

In the dVRK system, the clutch is engaged with a foot pedal or a button accessible by the index finger. However, the current rotation of the tool is maintained and cannot be changed (this is achieved by blocking the last two joints of the controller). In contrast, our system implements full clutching (both translation and rotation). The clutch is engaged by closing the hand (**Fist** gesture) as described next.

The clutching mechanism includes 3 phases:

Leading Edge: When the **Fist** gesture is detected, the clutch is engaged, and the vibrotactile feedback of the glove is activated. The current configuration of the PSM g_r^0 is recorded and the robot is prevented from moving. Note that the jaw of the instrument is allowed to move.

Active Clutch: The vibrotactile feedback continues to be activated. The PSM is held immobile. The glove can be moved to an arbitrary pose, allowing the user to move to a comfortable configuration.

Hand Gesture	Representation	Hand Gesture	Representation
Thumbs up		Pinky	
Ring		Fist	

TABLE I: Gestures trained for distinct functionalities. In this paper, **Fist** invokes the clutch mechanism and **Ring** toggles the robot control on or off. **None** gesture corresponds to the case when the subject is not using any of the four gestures above.

Trailing Edge: When the gesture becomes other than **Fist**, the clutch is disengaged and the vibrotactile feedback is deactivated. The tracker frame H and the tracker base frame S are aligned, and their axes are aligned with the axes of the PSM tip frame T whose configuration is described by g_r^0 .

III. HAND GESTURE RECOGNITION

To train the classifiers for hand gesture recognition, we created a custom dataset. We used 5 sets of approximately 3 – 5 minute recordings from the glove worn by one of the authors while performing one of the 4 gestures reported in Table I, or none of them. The recorded data (Table II) consists of the point cloud of each of the 21 landmark relative poses (3 position entries and 4 quaternion entries) regarding the wrist IMU (147 features). Table III shows examples of point clouds for different gestures. Each recording has been made while changing the position and orientation of the hand as much as possible to ensure the widest variety of data. Each recording corresponds to one gesture (or no gesture) so when merging all the data it was easy to attribute a class to each sample. As the number of classes is small, a simple one-hot encoding has been used.

Hand Gesture	None	Pinky	Ring	Fist	Thumbs up
Train set	20743	12833	25011	16738	19447
Test set	4167	2493	5075	3445	3775

TABLE II: The size of our training and testing sets for hand gesture recognition.

A. Classifiers

We initially used Random Forests (RF) [22] as a model for gesture recognition. Subsequently, we explored the Multilayer Perceptron (MLP) classifier [23]. The MLP model was configured with two hidden layers containing 40 and 25 neurons, respectively, and a maximum of 100 iterations. The use of such a small model with only two hidden layers helps prevent overfitting.

In addition to these established models, we investigated a novel classifier, the Light Gradient Boosting Machine (L-GBM) [24]. L-GBM employs a sequential approach in which decision trees are added successively, with each tree

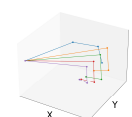
Input Hand Pose	Predicted Gesture	Input Hand Pose	Predicted Gesture
	Thumbs-up		Pinky
	Ring		Fist

TABLE III: Examples of point clouds used for gesture prediction.

correcting errors from the ensemble of preceding trees. Unlike traditional gradient-boosting methods, L-GBM directly minimizes the loss function. Tailored for efficient training on large datasets, it is particularly suitable for applications with resource constraints, and it can quickly predict data.

We also trained a Histogram-based Gradient Boosting model that combines the traditional gradient boosting [25] and the histogram-based algorithm [24]. Unlike traditional gradient boosting methods that operate on individual data points, histogram-based gradient boosting works with binned feature values. By constructing histograms of input features, this approach accelerates the computation of information gained during tree construction. The binning process reduces the number of unique feature values, resulting in faster training times and decreased memory usage.

B. Results

By training the models above, it is possible to recognize 5 different gestures (tested on a new, unseen dataset). The models were implemented in ROS and Table IV shows their performance. The confusion matrices for each model are shown in Fig. 2.

Model	Accuracy	F1 Score	Recall
MLP	0.9852	0.9852	0.9852
L-GBM	0.9508	0.9505	0.9508
RF	0.9417	0.9413	0.9417
HGBT	0.9628	0.9627	0.9628

TABLE IV: Evaluation metrics for the trained models.

Although all models exhibited high accuracy, F1 scores, and recall, we selected the MLP model for implementation due to its high prediction speed (Table V) and high accuracy. The average frequency at which the MLP model can operate (determined from the ROS logs) is around 96Hz. From Fig. 2, it is noticeable that the **Pinky** and **Ring** gestures are associated with more errors. This observation can be attributed to the similarity between these two gestures.

In our application, gesture recognition needs to be performed continuously and in real-time. To ensure the stability of recognition – for example, even a single mistake in the clutch could lead to problematic input sent to the robot –

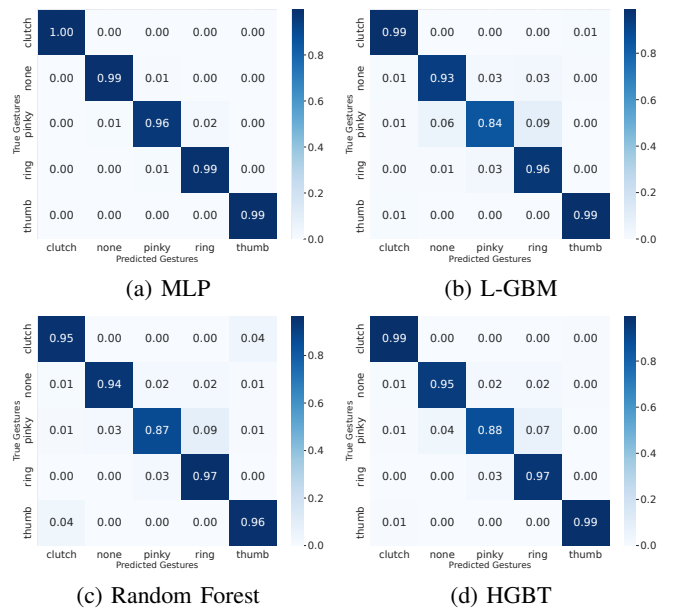


Fig. 2: Confusion matrices for gesture recognition models.

Model	Mean Time (ms)	Std. Deviation (ms)
MLP	0.75	0.14
L-GBM	2.09	3.06
RF	0.92	0.16
HGBT	7.81	4.72

TABLE V: Prediction time for each model (1000 trials).

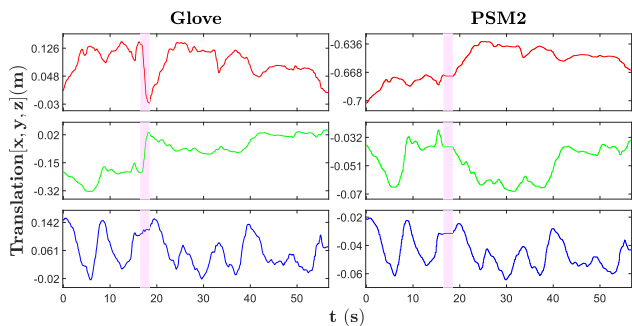
we use a sliding window of length 7. The predictions of the MLP model over the last 7 time steps are stored in a 7x5 matrix, with each row corresponding to a time sample and each column representing a gesture prediction (0 or 1). The matrix is initialized with zeros. During each iteration, a new row is added with the most probable gesture set to one; the oldest prediction is deleted from the matrix. Finally, in each iteration, the system selects the gesture with the highest column sum. This induces a negligible delay but greatly increases the stability of the prediction.

IV. PRELIMINARY EVALUATION

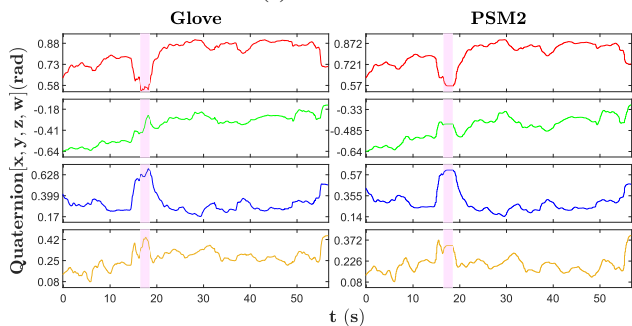
To evaluate the system, the members of the team with surgical training were asked to use the system to complete one of the standard da Vinci training exercises [26]. The original exercise was modified to suit our system’s single-arm setup and to simplify the task, thereby reducing any uncertainties in the preliminary test. The modified task required participants to control the PSM with their left hand to lift a peg from one pin on the pegboard and transfer it to another pin. One trial consists of repeating this task twice with two different pegs on the pegboard.

A. Experiment Setup

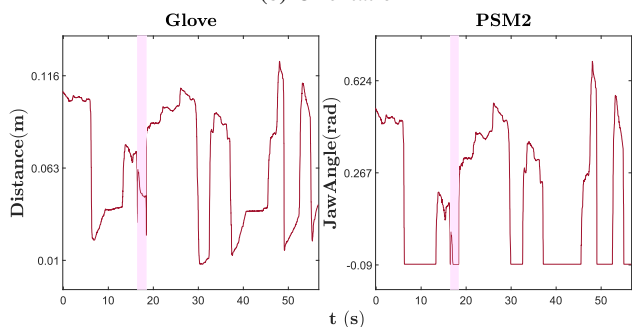
The experimental setup is shown in Fig. 1. The user’s hand starts in a position similar to that shown in the figure, away from the robot. The endoscopy was positioned to allow a view of the pegs on the board and the tip of the instrument. God Vision glasses were connected to the



(a) Translation



(b) Orientation



(c) Jaw Movements

Fig. 3: A sample recording of motion between the glove and the PSM. The segments highlighted in purple indicate periods when the clutch mechanism was engaged. (a) displays the translation of the glove and PSM while (b) shows the orientation of the glove and PSM respectively. (c) compares the distance of the thumb and index finger on the glove with the jaw angle of the PSM.

vision tower, and the user wore the glasses to access the stereo endoscopic view. The evaluation was carried out by 5 surgeons and one fellow, all members of the research team. All have prior experience with the da Vinci surgical console to perform surgical tasks. Participants underwent a brief training session, lasting approximately 2 to 10 minutes, primarily to familiarize themselves with the operation of the clutch mechanism. Each participant performed the exercise 5 times. To implement our system, we needed to update the dVRK. This caused compatibility issues with the existing dVRK console so we were not able to conduct the exercise through the standard da Vinci console.

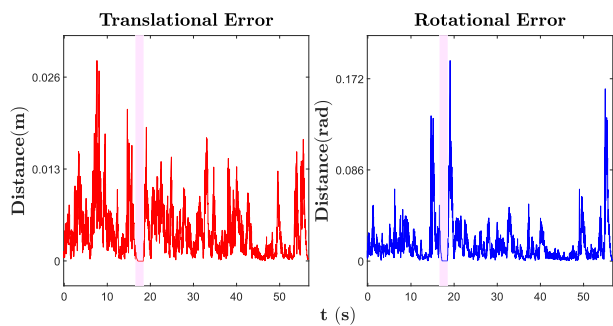


Fig. 4: Translational and orientational distance between the glove and the PSM: the left figure depicts the Euclidean distance, while the right one details the orientation difference, quantified with rotation matrices (in the hand workspace).

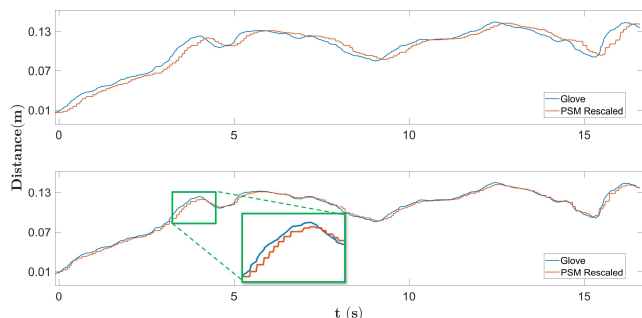


Fig. 5: Both plots detail the x-axis translation of the glove and the PSM tip in Fig. 3a. The initial plot illustrates a delay in the robot's execution of the glove's movements. To address this, the delay between the signals was measured based on the peaks, and the aligned signals were shown on the bottom.

B. Control Results

A sample trajectory of the da Vinci arm controlled with our proposed glove, performed by one of the surgeons, is shown in Fig. 3. A comparison of the kinematics of the glove and the instrument tip is shown in Figs. 3a and 3b, respectively. The motion of the PSM exhibits a stair-case movement due to the implementation of position control of the arm in dVRK (green box in Fig. 5), where the robot temporarily stops once it reaches the goal position. The shaded regions show the moments when the clutch (**Fist** gesture) was activated. Our clutch mechanism (Section II-G) prevents the PSM from moving while activated and resumes the movement smoothly when released. The motion of the index and thumb of the glove and the instrument jaw is depicted in Fig. 3c. Currently, the fully closed configuration of the FBF jaw is represented by a negative value in the dVRK's system (as the 0° angle corresponds to a parallel configuration of the jaw where it is not completely closed); the slight difference for extreme values between the glove and the PSM is due to the scaling between the glove and the jaw.

To compare the input motion of the glove and the output motion of the instrument tip, we first reversed the scaling (the inverse of Eq. (1)) of the movement of the instrument tip (Fig. 5). The figure clearly shows a delay between the

two trajectories, mainly due to the computation time for the inverse kinematics. To accurately estimate the error between the input and output signals and eliminate the effect of the delay, we identified the delay by the peak positions within each signal. Subsequently, the PSM signal is shifted according to the calculated delay to align with the glove’s signal (Fig. 5). The difference in translation was quantified using the Euclidean distance, while the discrepancy in rotation was determined using the standard bi-invariant metric on the group of rotations [27]. The errors derived from Figs. 3a and 3b are shown in Fig. 4. The duration and error metrics for each participant’s performance are depicted in Table VI. The average delay in all trials and all participants was 0.223s.

User	Average Duration (s)	Translational Error (m)		Rotational Error (rad)	
		Average	Std. dev.	Average	Std. dev.
A	60.345	0.005	0.004	0.024	0.024
B	45.304	0.004	0.004	0.016	0.018
C	57.922	0.005	0.004	0.040	0.056
D	53.298	0.004	0.004	0.021	0.026
E	52.506	0.003	0.003	0.015	0.015
F	37.782	0.003	0.003	0.021	0.021

TABLE VI: the first column displays the average runtime for the five trials. The subsequent columns detail the overall mean and standard deviation of the errors, calculated based on the glove’s workspace, performed by each participant (complete version available on [28]).

C. Survey Results

In the follow-up survey, each participant was asked five questions: 1) How comfortable was the glove controller? 2) How responsive was the robot when controlled with the glove controller? 3) How intuitive was controlling the jaw with your fingers? 4) How intuitive was it to control the arm with the glove? 5) Was the vibrotactile feedback for the clutch effective? We use a 7-point Likert scale for the response, with 7 being the most positive response [29]. The average responses for the 6 participants are summarized in Table VII. The results of Questions 3 to 5 show that the new control architecture is intuitive. This is further evidenced by the small amount of practice required to complete the exercise. Questions 1 and 2 produced satisfactory results; all participants responded that the system was ‘highly responsive.’ However, the results of Question 1 indicate that the overall ergonomics of the system can be improved, as most users had to lift their elbow to achieve a correct angle with their hand. This issue also highlights two important aspects: first, the user’s experience with the device may significantly impact their comfort, as they can readjust themselves by clutching to find a better position. Second, an ergonomic seat can greatly reduce the user’s effort.

Question #	Q1	Q2	Q3	Q4	Q5
Avg. Score	5.50	6.00	6.50	6.50	6.33

TABLE VII: Average scores in the Likert scale from the users.

V. CONCLUSION

This paper presents a novel user interface for the da Vinci surgical robot arm. The system integrates the Manus Meta Prime 3 Haptic XR glove, the HTC Vive Tracker, God Vision wireless smart glasses, and controls one arm of the dVRK surgical robot platform. In addition to moving the arm, the surgeon can use fingers to control the end-effector of the surgical instrument. A custom robot calibration was implemented to address the inherent inaccuracies of the dVRK system. A combination of scaling and gesture recognition was used to achieve precise and intuitive control of the robot’s movements while implementing an upgraded version of the clutch mechanism. In particular, we introduced clutching of the instrument orientation, a functionality not available in the da Vinci system. The vibrotactile elements of the glove are used to provide feedback to the user when gesture commands are invoked.

The proposed interface offers several potential advantages. Surgeons can directly control robotic arms by moving their hands, without the need for additional physical devices. This facilitates a more immersive surgeon-robot interaction. However, it should be noted that the hardware used in our setup is not the latest available on the market; we used the first version of HTC Vive Trackers and Manus Meta Prime 3 XR, both of which have lower precision compared to their upgraded versions (HTC Vive Trackers v2 and Quantum XR Metaglove).

The system was tested by members of the team with surgical training, including 5 surgeons and 1 fellow. They were asked to perform a surgical training task similar to those used in training with the da Vinci devices. The evaluation shows that the system is responsive and precise. Surgeons were able to effectively complete training exercises with minimal practice with the new interface, suggesting that the interface is highly intuitive. After the exercise, each participant filled out a questionnaire to provide feedback on their user experience. The responses show a high level of user satisfaction.

Existing surgical consoles are bulky and take up valuable space. They limit the ability to optimize the operating room setup for throughput. They also pose challenges to the communication of the surgical team, leading to potential workflow disruptions. In contrast, our proposed system is inexpensive as it uses off-the-shelf components, and it dramatically reduces space requirements. It demonstrates how modalities such as vibrotactile feedback can efficiently provide additional information to the surgeon without cluttering the visual field. Finally, the proposed architecture allows for rapid prototyping and opens opportunities for further innovations in the design of surgical robot interfaces.

Future work includes implementing velocity control to enhance user experience, upgrading hardware to improve tracking precision, enabling full control for the right hand, and expanding the repertoire of user gestures to increase the range of available actions.

REFERENCES

- [1] F. Kanji, T. Cohen, M. Alfred, A. Caron, S. Lawton, S. Savage, D. Shouhed, J. T. Anger, and K. Catchpole, "Room size influences flow in robotic-assisted surgery," *International Journal of Environmental Research and Public Health*, vol. 18, no. 15, p. 7984, 2021.
- [2] R. Bharathan, R. Aggarwal, and A. Darzi, "Operating room of the future," *Best Practice & Research Clinical Obstetrics & Gynaecology*, vol. 27, no. 3, pp. 311–322, 2013.
- [3] W. S. Sandberg, B. Daily, M. Egan, J. E. Stahl, J. M. Goldman, R. A. Wiklund, and D. Rattner, "Deliberate perioperative systems design improves operating room throughput," *The Journal of the American Society of Anesthesiologists*, vol. 103, no. 2, pp. 406–418, 2005.
- [4] J. E. Stahl, W. S. Sandberg, B. Daily, R. Wiklund, M. T. Egan, J. M. Goldman, K. B. Isaacson, S. Gazelle, and D. W. Rattner, "Reorganizing patient care and workflow in the operating room: a cost-effectiveness study," *Surgery*, vol. 139, no. 6, pp. 717–728, 2006.
- [5] A. Simorov, R. S. Otte, C. M. Kopietz, and D. Oleynikov, "Review of surgical robotics user interface: What is the best way to control robotic surgery?" *Surgical Endoscopy*, vol. 26, no. 8, pp. 2117–2125, Aug. 2012.
- [6] L. Cofran, T. Cohen, M. Alfred, F. Kanji, E. Choi, S. Savage, J. Anger, and K. Catchpole, "Barriers to safety and efficiency in robotic surgery docking," *Surgical endoscopy*, pp. 1–10, 2021.
- [7] N. Hong, M. Kim, C. Lee, and S. Kim, "Head-mounted interface for intuitive vision control and continuous surgical operation in a surgical robot system," *Medical & Biological Engineering & Computing*, vol. 57, no. 3, pp. 601–614, Mar. 2019.
- [8] R. Wen, W.-L. Tay, B. P. Nguyen, C.-B. Chng, and C.-K. Chui, "Hand gesture guided robot-assisted surgery based on a direct augmented reality interface," *Computer Methods and Programs in Biomedicine*, vol. 116, no. 2, pp. 68–80, Sep. 2014.
- [9] X. MercilinRaajini, S. Abirami, S. Keerthana, N. Shrivastava, N. Malokhat, and R. Yokeshwaran, "Mem based hand gesture controlled wireless robot," in *E3S Web of Conferences*, vol. 399. EDP Sciences, 2023, p. 01013.
- [10] M. K. Burns and R. Vinjamuri, "Design of a soft glove-based robotic hand exoskeleton with embedded synergies," *Advances in Motor Neuroprostheses*, pp. 71–87, 2020.
- [11] A. Brygo, I. Sarakoglou, G. Grioli, and N. Tsarakakis, "Synergy-based bilateral port: A universal control module for tele-manipulation frameworks using asymmetric master-slave systems," *Frontiers in bioengineering and biotechnology*, vol. 5, p. 19, 2017.
- [12] HTC Vive, *HTC Vive Tracker Developer Guidelines*. HTC Vive, 2020. [Online]. Available: <https://developer.vive.com/documents/721/HTC-Vive-Tracker-2018-Developer-Guidelines-V1.pdf>
- [13] MANUS, *MANUS Prime 3 Haptic XR full spec sheet*. MANUS, 2021. [Online]. Available: [https://assets.website-files.com/61de97d15a7bb6441d9565c0/65127f073666b95695695832c32_DataSheet%20-%20Prime%203%20Haptic%20XR%20\(small\).pdf](https://assets.website-files.com/61de97d15a7bb6441d9565c0/65127f073666b95695695832c32_DataSheet%20-%20Prime%203%20Haptic%20XR%20(small).pdf)
- [14] P. Kazanzides, Z. Chen, A. Deguet, G. S. Fischer, R. H. Taylor, and S. P. DiMaio, "An open-source research kit for the da Vinci surgical system," in *IEEE Intl. Conf. on Robotics and Auto. (ICRA)*, Hong Kong, China, 2014, pp. 6434–6439.
- [15] MediThinkQ, *GV-200D Catalog*. MediThinkQ, 2019. [Online]. Available: <https://s3.ap-northeast-2.amazonaws.com/logicsquare-seoul/b56c22db-7a69-4e28-868-8827/c4/1d0e/cv-200d%20ENG%20Catalog.pdf>
- [16] Open Source Robotics Foundation, "Robot operating system." [Online]. Available: <https://www.ros.org>
- [17] K.-H. Oh, L. Borgioli, M. Zefran, L. Chen, and P. C. Giulianotti, "A framework for automated dissection along tissue boundary," 2023. [Online]. Available: <https://arxiv.org/abs/2310.09669>
- [18] O. Kreylos, "Lighthouse tracking examined," *Doc-ok.org*, vol. 25, p. 12, 2016.
- [19] D. C. Niehorster, L. Li, and M. Lappe, "The accuracy and precision of position and orientation tracking in the htc vive virtual reality system for scientific research," *i-Perception*, vol. 8, no. 3, p. 2041669517708205, 2017.
- [20] V. Bazarevsky, Y. Golubev, Y. Kartynnik *et al.*, "MediPIPE: A framework for building perception pipes," *arXiv preprint arXiv:1906.08172*, 2019.
- [21] K.-H. Oh, L. Borgioli, A. Mangano, V. Valle, M. D. Pangrazio, F. Toti, G. Pozza, L. Ambrosini, A. Ducas, M. Zefran, L. Chen, and P. C. Giulianotti, "Comprehensive robotic cholecystectomy dataset (crcd): Integrating kinematics, pedal signals, and endoscopic videos," 2023. [Online]. Available: <https://arxiv.org/abs/2312.01183>
- [22] L. Breiman, "Random forests," *Machine learning*, vol. 45, pp. 5–32, 2001.
- [23] G. E. Hinton, "Connectionist learning procedures," in *Machine learning*. Elsevier, 1990, pp. 555–610.
- [24] G. Ke, Q. Meng, T. Finley, T. Wang, W. Chen, W. Ma, Q. Ye, and T.-Y. Liu, "Lightgbm: A highly efficient gradient boosting decision tree," in *Advances in Neural Information Processing Systems*, I. Guyon, U. V. Luxburg, S. Bengio, H. Wallach, R. Fergus, S. Vishwanathan, and R. Garnett, Eds., vol. 30. Curran Associates, Inc., 2017. [Online]. Available: https://proceedings.neurips.cc/paper_files/paper/2017/file/6449f44a102fde848669bdd9e
- [25] J. H. Friedman, "Stochastic gradient boosting," *Computational statistics & data analysis*, vol. 38, no. 4, pp. 367–378, 2002.
- [26] A. M. Derossis, G. M. Fried, M. Abrahamowicz, H. H. Sigman, J. S. Barkun, and J. L. Meakins, "Development of a model for training and evaluation of laparoscopic skills 11this work was supported by an educational grant from united states surgical corporation (auto suture canada)." *The American Journal of Surgery*, vol. 175, no. 6, pp. 482–487, 1998. [Online]. Available: <https://www.sciencedirect.com/science/article/pii/S0002961098000804>
- [27] M. Zefran, V. Kumar, and C. Croke, "Metrics and Connections for Rigid-Body Kinematics," *The International Journal of Robotics Research*, vol. 18, no. 2, pp. 242–1, Feb. 1999.
- [28] L. Borgioli, K.-H. Oh *et al.*, "Sensory glove-based surgical robot user interface," 2024. [Online]. Available: <https://uofi.box.com/s/lnslb5xqvzvok3p0gcy01er1o6dwhqio>
- [29] M. Schrum, M. Ghuy, E. Hedlund-Botti, M. Natarajan, M. Johnson, and M. Gombolay, "Concerning trends in likert scale usage in human-robot interaction: Towards improving best practices," *J. Hum.-Robot Interact.*, vol. 12, no. 3, apr 2023. [Online]. Available: <https://doi.org/10.1145/3572784>
- [30] F. Pedregosa, G. Varoquaux, A. Gramfort, V. Michel, B. Thirion, O. Grisel, M. Blondel, P. Prettenhofer, R. Weiss, V. Dubourg, J. Vanderplas, A. Passos, D. Cournapeau, M. Brucher, M. Perrot, and E. Duchesnay, "Scikit-learn: Machine learning in Python," *Journal of Machine Learning Research*, vol. 12, pp. 2825–2830, 2011.
- [31] D. Zhang, J. Liu, L. Zhang, and G.-Z. Yang, "Hamlyn crm: A compact master manipulator for surgical robot remote control," *International journal of computer assisted radiology and surgery*, vol. 15, pp. 503–514, 2020.
- [32] Y. Sheng, H. Cheng, Y. Wang, H. Zhao, and H. Ding, "Teleoperated surgical robot with adaptive interactive control architecture for tissue identification," *Bioengineering (Basel)*, vol. 10, no. 10, p. 1157, Oct 2023.
- [33] H. Sakoe and S. Chiba, "Dynamic programming algorithm optimization for spoken word recognition," *IEEE Transactions on Acoustics, Speech, and Signal Processing*, vol. 26, no. 1, pp. 43–49, 1978.
- [34] S. Calinon, D. Bruno, M. S. Malekzadeh, T. Nanayakkara, and D. G. Caldwell, "Human-robot skills transfer interfaces for a flexible surgical robot," *Computer Methods and Programs in Biomedicine*, vol. 116, no. 2, pp. 81–96, Sep. 2014.
- [35] A. D. Greer, P. M. Newhook, and G. R. Sutherland, "Human-Machine Interface for Robotic Surgery and Stereotaxy," *IEEE/ASME Transactions on Mechatronics*, vol. 13, no. 3, pp. 355–361, Jun. 2008.
- [36] L. Prokhorenko, D. Klimov, D. Mishchenkov, and Y. Poduraev, "Surgical robot interface development framework," *Computers in Biology and Medicine*, vol. 120, p. 103717, May 2020.
- [37] T. Yamamoto, N. Abolhassani, S. Jung, A. M. Okamura, and T. N. Judkins, "Augmented reality and haptic interfaces for robot-assisted surgery," *The International Journal of Medical Robotics and Computer Assisted Surgery*, vol. 8, no. 1, pp. 45–56, 2012.